ADVANCED OPTICAL MATERIALS
www.advopticalmat.de

# UV-Sensitive Wearable Devices for Colorimetric Monitoring of UV Exposure

*Wolfgang Kurz, Ali K. Yetisen,* Mihai Valer Kaito, Matthew J. Fuchter, Martin Jakobi, Martin Elsner, and Alexander W. Koch*

**The extensive exposure of the human epidermis to solar radiation creates a health risk that results in skin cancer. Commercial sunscreens offer sufficient protection from ultraviolet (UV) radiation; however, the ability to determine UV exposure limits can provide informed decisions about the dose of sunscreen required and the frequency of re-application. Here, a wide range of wearable devices that colorimetrically report on UV exposure are developed. Under UV radiation, UV-sensitive dyes change their color from 280 to 400 nm in the visible spectrum. By correlating the current color value and the UV dose, the amount of sun exposure is determined with an accuracy of 95%. A smartphone camera algorithm is coded to automatically perform the color analysis of these dyes. The UV-sensitive dyes are incorporated in wearable devices, skin patches, textiles, contact lenses, and tattoo inks. The developed wearable devices will ensure monitoring UV radiation to rationally manage the user's behavior in order to prevent harmful sun exposure.**

## 1. Introduction

Exposure to sunlight for long periods can lead to significant health problems including sunburn, premature skin aging, and skin cancer.[1] Ultraviolet (UV) rays in the sunlight are primarily responsible for skin damage and are categorized into UVA (400–320 nm), UVB (315–280 nm), and UVC (290–100 nm) rays,[2] where UVC is completely filtered by the ozone layer.[3] The consequential damages of sun exposure range from simple erythema to life-threatening skin cancers, resulting in high-cost protracted medical therapies.[4] The harmless amount of UVA and UVB can be determined by using a protective agent according to the individual's skin type and radiation exposure intensity. Current protective methods such as sunscreens, UV-weakening or UV-impermeable clothing offers sufficient protection against UV-radiation. However, these approaches do not provide any information about the UV-radiation threshold that damages the epidermis.

Present portable technologies that measure personal UV radiation are usually based on miniaturized electronic components with power supply.[5] These dosimeters consist of a photodiode detector that generates digital signals that represent the irradiance.[6] However, individual calibration of device and optimal alignment of the sensor to the incoming solar radiation are required to achieve accurate results, as the sensor sensitivity decreases due to the angular deviation. The calibration of the sensor as a dosimeter to the erythema weighted function is required to estimate the biological effects caused by UVB radiation.[7] However, these dosimeters do not provide any information about the radiation limit during exposure. Recently, chemical UV dye compositions have been proposed to form color upon UV exposure.[8,9] These substances usually consist of a colorless precursor and a UV-sensitive trigger.

Here, we developed a wide range of wearable devices that report on the personal UVA and UVB radiation dose in real-time. These devices employ UV-sensitive dyes that undergo a chemical reaction upon irradiation, which in turn generates a colored dye as indicator to provide a signal for readout. To quantify UVA and UVB dose variations in the dyes, a smartphone algorithm was developed to convert the CMOS data into UV dose values. The combination of UV-sensitive oxidant and indicator dye were incorporated in wearable devices including skin patches, textiles, contact lenses and tattoo inks. These portable devices operated without any electronic components to monitor the user's received UV-radiation.

## 2. Results and Discussion

Upon irradiation, the photosensitive agent (a triphenylsulfonium or diphenyliodonium ion) triggers a hydride transfer from

W. Kurz, A. K. Yetisen, M. V. Kaito, M. Jakobi, A. W. Koch
Institute for Measurement Systems and Sensor Technology
Technical University of Munich
80333 Munich, Germany
E-mail: a.k.yetisen@tum.de
M. J. Fuchter
Department of Chemistry
Imperial College London
Molecular Sciences Research Hub
White City Campus, Wood Lane, London W12 0BZ, UK
M. Elsner
Chair of Analytical Chemistry and Water Chemistry
Technical University of Munich
81377 Munich, Germany
The ORCID identification number(s) for the author(s) of this article can be found under https://doi.org/10.1002/adom.201901969.



**DOI: 10.1002/adom.201901969**

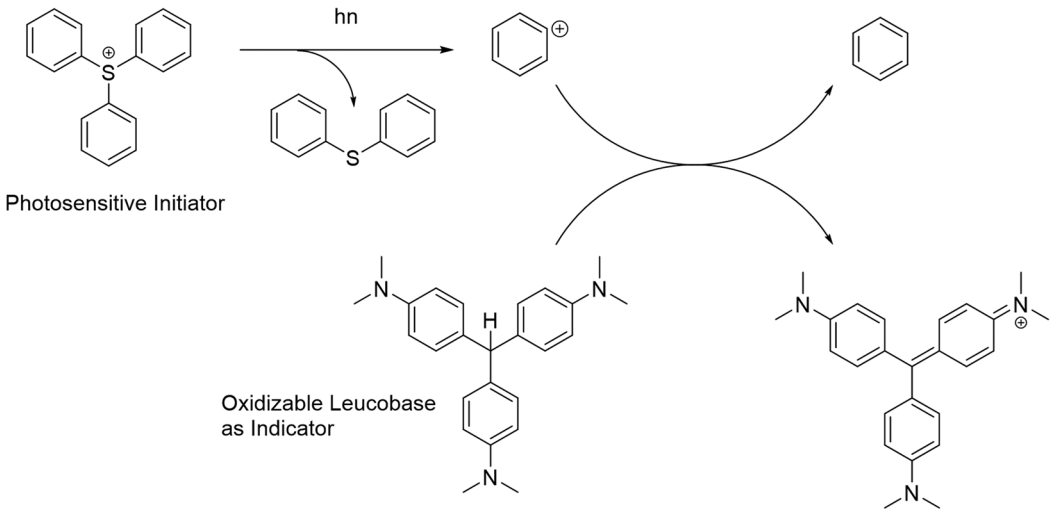


**Figure 1.** Process of color change of a leucobase (tris(4-(*N*,*N*-dimethylamino)phenyl)methane, Leuco Crystal Violet) upon irradiation-triggered decomposition of a photosensitive initiator (an example of decomposition of triphenylsulfonium ions to aryl cations). These short-lived carbenium ions are known to produce $H^+$ ions with solvents or water.[11] They effectuate a hydride transfer to oxidize the leucobase and generate the observed color change.

the triphenylmethyl dye (a p-aminophenyl)methyl leucobase) so that the leucobase is transformed from its amino to its imino form and changes color. **Figure 1** shows the process of color change for the example of triphenylsulfonium as photosensitive initiator and tris(4-(*N*,*N*-dimethylamino)phenyl)methane (Leuco Crystal Violet) as oxidizable indicator. Further irradiation results in photodegradation as the chemical structure of these dyes is destructed.[10] Through this controllable oxidation by selective irradiation with light of different intensities and duration, the color conversion can be precisely controlled and therefore provides accurate visual colorimetric data about the UV light exposure and duration.

To assess the functionality of UV sensitive dyes as a dosimeter, the samples were irradiated with UVA/-B and D65 light sources to induce a color change. The reflected radiation of the samples was measured by a spectrometer (360–830 nm).[12] Four different samples were tested, two liquid ones IS300 and IS101 as well as two self-adhesive labels H and S (designation according to manufacturer). **Figure 2** illustrates the measurement results for IS300 dye sample, which changes color from yellow to green upon UV exposure. Figure 2a shows the spectral distribution of IS300 dye as a function of time for a radiation intensity of 50.4 mW $m^{-2}$. Prior to UV exposure, a spectral broadband peak at 580–600 nm resulted in yellow color. With continuous UV irradiation, the broadband peak diminished and two maxima at 510 and 660 nm remained. Since the human eye has a low sensitivity for light at longer wavelengths,[13] the latter maxima had no influence on human perception. Hence, the color of the UV dye was determined by the first peak, representing a green color. The color course as a function of time (30 min) is presented in the CIE 1931 color space (Figure 2b). IS300 dye shifted its initial from yellow to green color as the UV exposure duration increased. Figure 2c illustrates the color gradient change under a constant UV light exposure in the RGB channels, where the value 255 represents the maximum color portion in 8-bit format. The red and green values were significantly higher than the blue value, and therefore a combination of these RGB values produced a yellow color. After 30 min of UV irradiation, the UV-sensitive dye formed a green color, with the green value as the strongest channel. Figure 2d illustrates the color gradient from yellow to green of IS300 sample by displaying the respective color components (representative wavelength components). Prior to UV exposure, the intensity of the yellow component was the highest in the spectrum. After 2 min of UV exposure, the yellow component decreased and the green component became dominant. The intensities of both components decreased over time, resulting in a loss of brightness. To demonstrate the transformation speed of the color as a function of intensity, the sample was irradiated at 37.0, 50.4, 70.5, and 85.0 mW $m^{-2}$ (Figure 2e). With increasing UV light exposure intensity, the photochemical process accelerated to rapidly form the yellow color. UV exposure of 37.0 mW $m^{-2}$ resulted in the slowest reflection intensity decrease. With increasing UV exposure intensity (85.0 mW $m^{-2}$), the reflection intensity decrease became steeper. Figure 2f shows the photographs of the dye as a function of UV light exposure intensity and time.

**Figure 3** presents the measurement results of the UV sensitive dye IS101 with a color change from transparent/white to blue. The reflected spectrum in Figure 3a shows a spectral distribution over the entire visible range without exposure to UV-radiation, which is representative of a white perception. With continuous irradiation, the spectrum decreases and two peaks at 480 and 680 nm appear, whereas the second maximum is also neglected due to the sensitivity of human perception, and blue is the corresponding color. Figure 3b demonstrates the color gradient and shows a clear shift from white to blue of the UV-dye with increasing exposure duration. The RGB-components (Figure 3c) confirm the color change, while at the beginning all three RGB values are similar indicating white but with progressing time the red value drops toward zero and also the

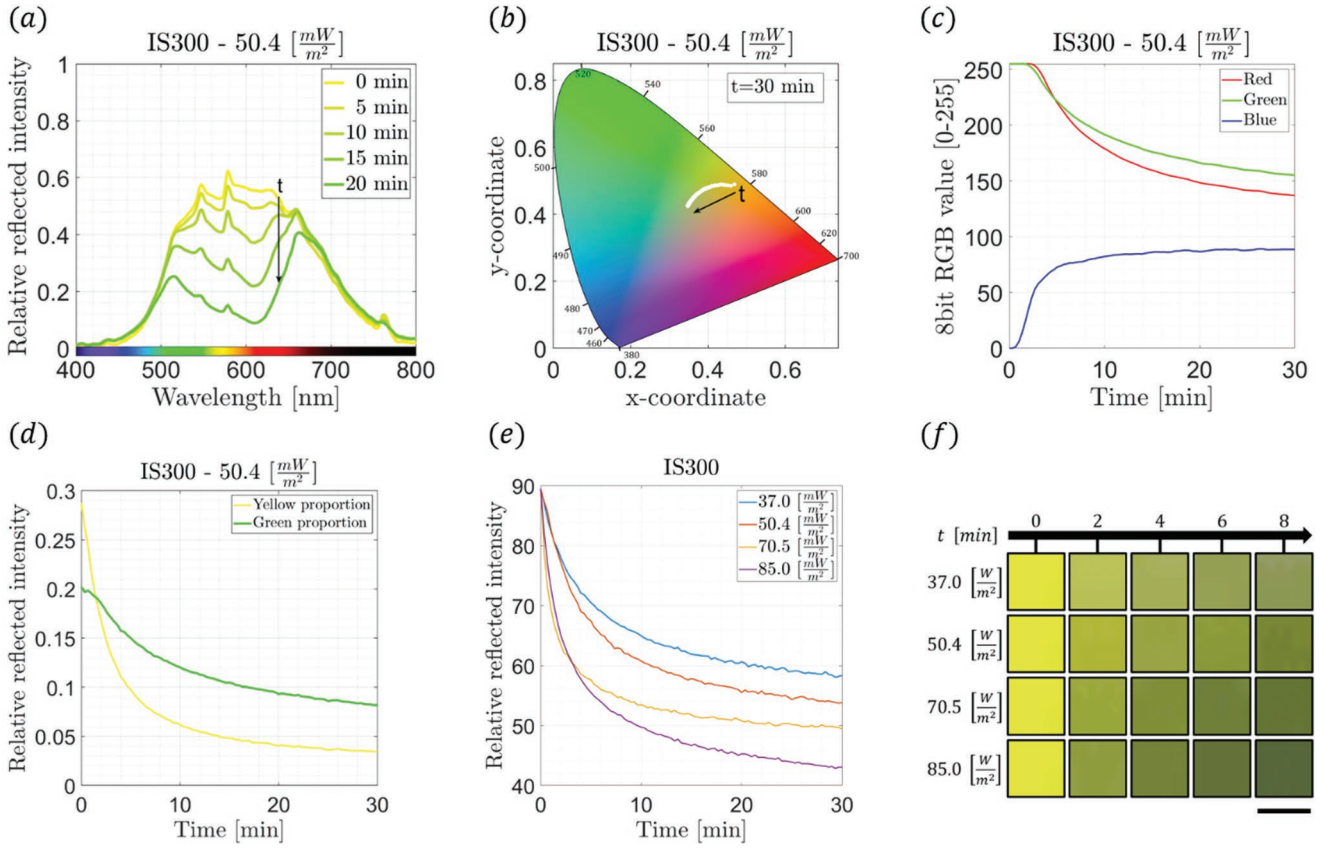


**Figure 2.** Measurement results of the UV-sensitive IS300 dye. a) Spectral distribution of the reflected colors as a function of time under a constant UV irradiation intensity of 50.4 mW $m^{-2}$. b) Color gradient change of the dye in the CIE 1931 color space from yellow to green color as a function of UV light exposure time. c) Temporal progression of the RGB-components as 8-bit values as a function of time under a constant UV light exposure. d) Wavelength ranges of the dye for specific colors (yellow: 570–590 nm and green: 500–540 nm) as a function of time. e) Color gradient change over time at 37.0, 50.4, 70.5, and 85.0 mW $m^{-2}$. f) Photographs of color gradient change over time at 37.0, 50.4, 70.5, and 85.0 mW $m^{-2}$ UV light exposure. Scale bar = 10 mm.

green value decreases significantly while the blue value remains quite constant. Figure 3d affirms the results of Figure 3c and shows that primarily the blue component is present toward the end of the color change process. The results in Figure 3e of IS101 indicate the relationship of intensity and the rate of color forming and therefore the color change is performed the fastest at the highest intensity of irradiation (85.0 mW $m^{-2}$ purple graph) and with decreasing intensity also the process speed decreases in the same manner. The visual representation of IS101 in Figure 3f verifies the relationship between the color-forming rate and intensity

The spectral distribution of the UV sensitive dye H in **Figure 4**a shows a decrease in intensity for wavelengths before 580 nm, resulting in a brown color forming upon UV exposure of the dye to its initial color white. The color gradient in the CIE 1931 color space (Figure 4b) of sample H illustrates the color forming from white to a brown tone. The red RGB component (Figure 4c) remains constant during irradiation with ultraviolet light, while the values of green and blue decrease in the same ratio for 200 min, proving the results of Figure 4b and this combination of RGB values result in a brown color of the UV-dye. Also, Figure 4d confirms these findings and shows a decrease in the wavelength proportion representative for white and brown, while the white proportion declines with a steeper gradient. The irradiation of the sample H with different intensities in Figure 4e describes the expected trend and shows a logical distribution from low to high respectively blue, red, yellow, and purple. Figure 4f also shows an accelerated color transformation with increasing intensity.

The reflected spectrum of the UV sensitive dye S is presented in **Figure 5**a and appears to have a white color without irradiation, but turns to purple color with continuous exposure. Two maxima are formed at 460 and at 660 nm. Since the second maximum is significantly greater than the first one, an influence on human perception is noted and this spectral distribution results in its distinctive color. The results in Figure 5b verify the outcome and a change to the purple color from its initial color white of sample S is seen. All three RGB components show a decrease over time, with the green component having the steepest drop following by the blue component. The red component has the highest value after irradiation and, in combination with the other components, results in purple color of sample S after irradiation with UV light. The compared proportions of white and purple of the reflected spectrum in Figure 5d

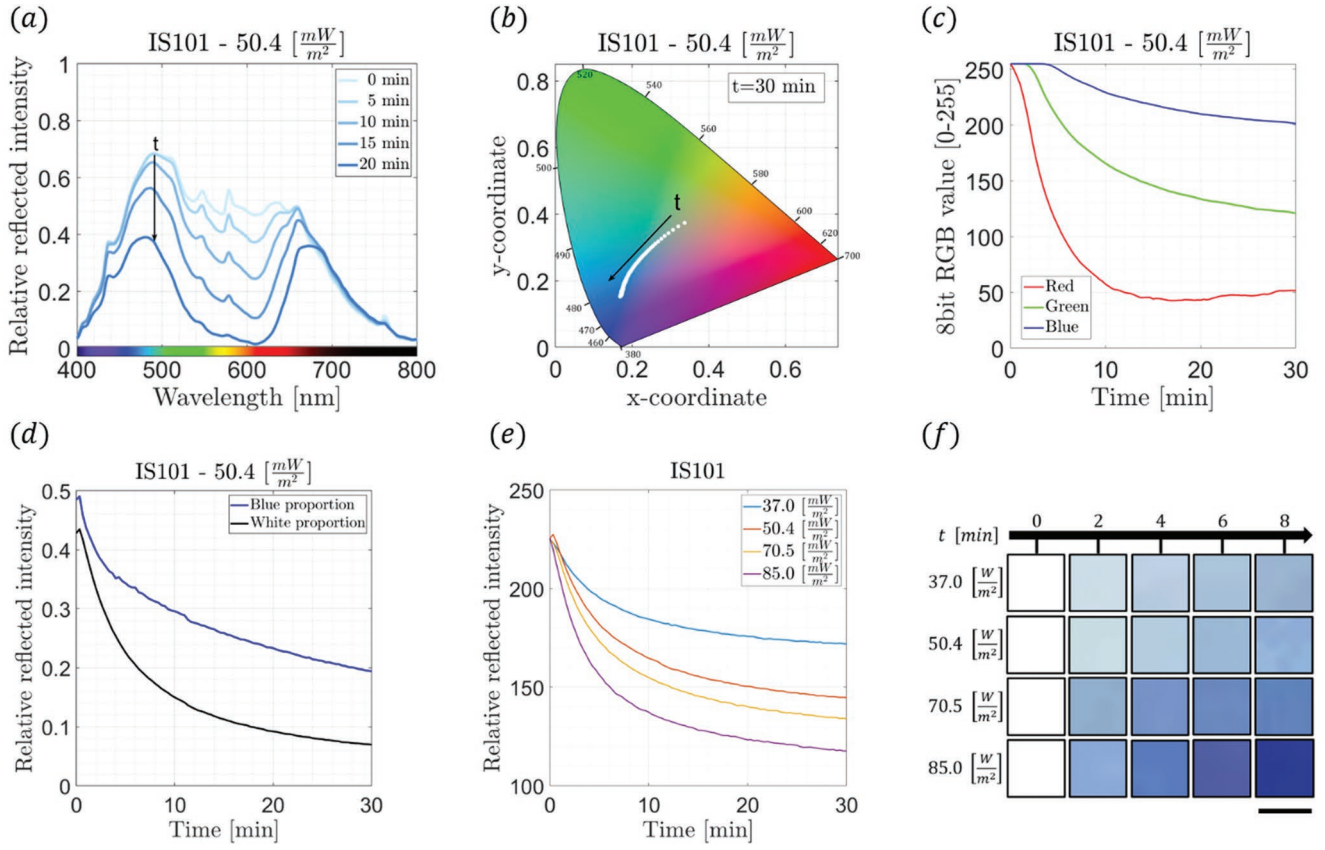


**Figure 3.** Measurement results of the UV-sensitive IS101 dye. a) Spectral distribution of the reflected colors as a function of time under a constant UV irradiation intensity of 50.4 mW $m^{-2}$. b) Color gradient change of the dye in the CIE 1931 color space from transparent/white to blue color as a function of UV light exposure time. c) Temporal progression of the RGB-components as 8-bit values as a function of time under a constant UV light exposure. d) Wavelength ranges of the dye for specific colors (transparent/white: 470–740 nm and blue: 400–500 nm) as a function of time. e) Color gradient change over time at 37.0, 50.4, 70.5, and 85.0 mW $m^{-2}$. f) Photographs of color gradient change over time at 37.0, 50.4, 70.5, and 85.0 mW $m^{-2}$ UV light exposure. Scale bar = 10 mm.

also prove that he purple proportion is more present toward the end. In Figure 5e a deviation for 50.4 mW $m^{-2}$ is recognizable and the red curve adapts to the yellow curve 70.5 mW $m^{-2}$, which suggests inaccuracies in the measurement setup. The other curves show the expected trend for a relationship between intensity and the color gradient rate. Nevertheless, the visual plots in Figure 5f prove the relationship of Figure 5e and the sample S shows at highest intensity also the highest saturation in color in the same duration. UV sensitive dyes showed clear color formation upon UV light exposure, depending on the UV light exposure intensity and time. This correlation enabled the assignment of the color changes of the respective UV dyes to the UV light irradiation dose or exposure time.

Due to a higher concentration of the photosensitive initiator, an accelerated color formation was noted (Figures 2–5e) and even low intensities (37 mW $m^{-2}$) were sufficient enough to trigger the chemical process (Figures 2–5f). Different angles of the light source directed to the sample showed the same effect in the reduction of the intensity, and thus color formation was still occurred with decreasing speed at increasing deviation. The tests also demonstrated longtime stability as the samples always had full transformation in color before degradation or photobleaching. Further tests should determine the sensitivity, the detection limit, and long-time stability.

## 3. UV-Sensitive Wearable Devices

Several wearable device models were implemented to demonstrate the versatile application of UV-sensitive dyes to monitor UV radiation exposure levels to prevent skin damage. The UV-dyes were integrated on a suitable substrate (polydimethylsiloxane, PDM[14]) and a protective film layer was applied on the dyes to conformably place the device on the target surface (curved plastic surface, epidermis, textile patch). The wristband consisted of a silicone strap with a 3D printed inlay element, which included the UV-sensitive dyes as well as two immutable colors with a protective layer (**Figure 6**a). The wristband was designed to enable automatic detection using machine learning. The scale on the wristband provided visual information about the current UV light exposure level. The wristband could be reused by replacing the irradiated 3D inlay with a new UV sensor unit. A textile patch was applied to a Velcro fastener and the UV-dyes were attached to synthetic leather protected by a film which could also be

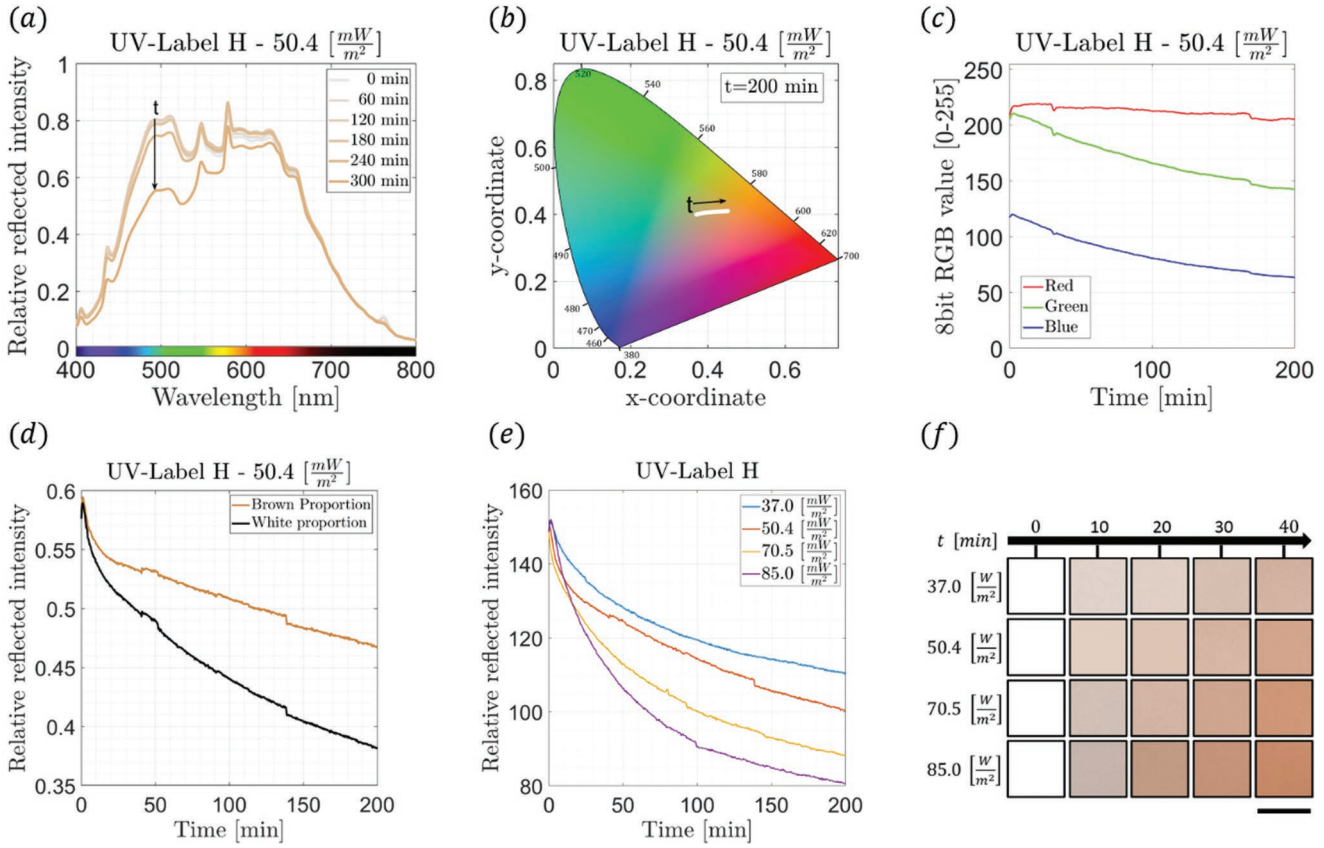


**Figure 4.** Measurement results of the UV-sensitive UV-Label H dye. a) Spectral distribution of the reflected colors as a function of time under a constant UV irradiation intensity of 50.4 mW $m^{-2}$. b) Color gradient change of the dye in the CIE 1931 color space from white to brown color as a function of UV light exposure time. c) Temporal progression of the RGB-components as 8-bit values as a function of time under a constant UV light exposure. d) Wavelength ranges of the dye for specific colors (white: 470–740 nm and brown: 550–740 nm) as a function of time. e) Color gradient change over time at 37.0, 50.4, 70.5, and 85.0 mW $m^{-2}$. f) Photographs of color gradient change over time at 37.0, 50.4, 70.5, and 85.0 mW $m^{-2}$ UV light exposure. Scale bar = 10 mm.

used as a UV blocker (Figure 6b). An additional scale for visual evaluation illustrated the current exposure for up to 1000 J $m^{-2}$, as minimal erythema dose (MED) can be chosen according to skin type.[15] This means, light skin types can produce sunburns already at 200 J $m^{-2}$ respectively 200 MED, whereas darker types endure doses up to 1000 MED (Figure S1, Supporting Information). The patch was applicable to any conformable surface. Figure 6c shows an epidermal skin patch containing a skin-adhesive plaster, UV dyes, and an optical patch. The top layer was waterproof. The conformable skin patch was suitable for outdoor use. When a sunscreen layer was applied on the skin patch, the color transformation slowed down depending on the sunscreen layer thickness and sun protection factor. Figure 6d demonstrates sunglasses based wearable device to display UV radiation exposure in athletes. Figure 6e shows the application of the UV-sensitive dyes in the form of tattoo inks, which were applied into the dermis by needle perforation. UV dyes were also deposited on a scleral lens to monitor UV radiation to prevent corneal damage or blindness (Figure 6f). These devices have applications in work safety, in particular, monitoring UV radiation exposure during welding and workplaces that involve highly intense laser sources. The user can recognize a color change in his visual field when a UV light exposure threshold is exceeded.

## 4. Quantification of UV Light Exposure with Smartphones

**Figure 7** shows the developed smartphone application that evaluates the color change of a UV-dye. After determining the user's irradiation dose (J $m^{-2}$), the application provides a guideline for skin protection. The home screen of the application allows the selection of different functions such as the scan of a UV-label to determine UV dosage, recommended protection methods, displaying the history of performed scans, and a diagnosis report (Figure 7a). In the first step, by selecting the scan function, the label to be scanned is chosen depending on the wearable device type: a bracelet, skin patch, contact lens, or a textile patch (Figure 7b). In the next step, the user's skin type is chosen to determine the specific MED, which defines the threshold for UV radiation damage (sunburns) (Figure 7c). Once these parameters are set, the camera interface of the smartphone is accessed to correct for color and brightness to compensate for ambient lighting conditions (Figure 7d). A UV label is scanned using the smartphone camera. The RGB color values of the UV dyes are extracted using object detection. A conversion into XYZ tristimulus values was computed using a predefined transformation matrix $M$

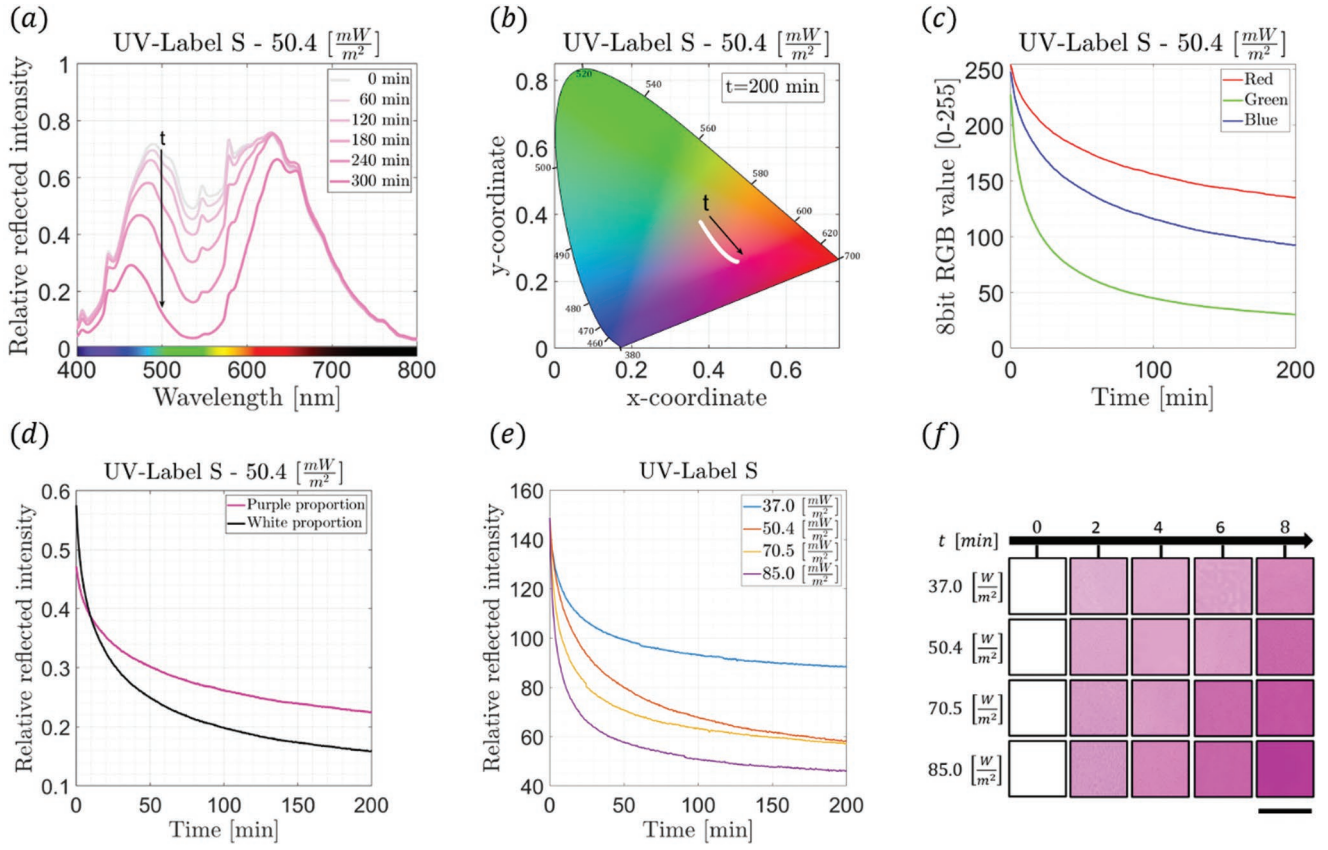


**Figure 5.** Measurement results of the UV-sensitive UV-Label S dye. a) Spectral distribution of the reflected colors as a function of time under a constant UV irradiation intensity of 50.4 mW $m^{-2}$. b) Color gradient change of the dye in the CIE 1931 color space from white to purple color as a function of UV light exposure time. c) Temporal progression of the RGB-components as 8-bit values as a function of time under a constant UV light exposure. d) Wavelength ranges of the dye for specific colors (white: 470–740 nm and purple: 590–740 nm) as a function of time. e) Color gradient change over time at 37.0, 50.4, 70.5, and 85.0 mW $m^{-2}$. f) Photographs of color gradient change over time at 37.0, 50.4, 70.5, and 85.0 mW $m^{-2}$ UV light exposure. Scale bar = 10 mm.

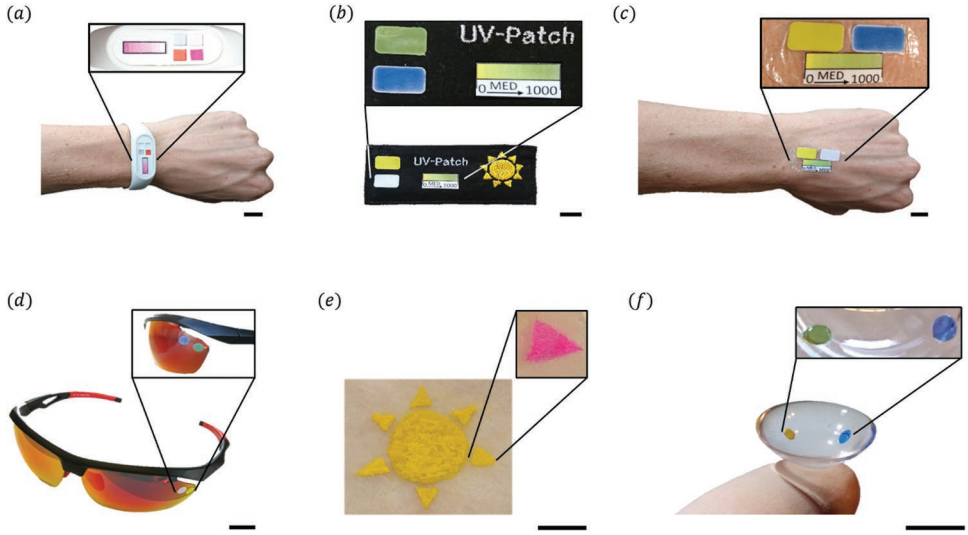


**Figure 6.** UV-sensitive wearable devices. a) Wristband containing a scale bar for visual readout of the dose and ambient light correction. b) Textile patch with a Velcro fastener and scale for visual readouts. c) Epidermal patch with an adhesive layer and a scale for visual readouts. d) Sunglasses with two types of UV- sensitive dyes. e) UV-dye integrated tattoos in the shape of the sun. f) Contact lens containing UV dyes. The insets show the status of the wearable devices prior to and after the UV exposure at 50.4 mW $m^{-2}$ for 30 min. Scale bars = 10 mm.

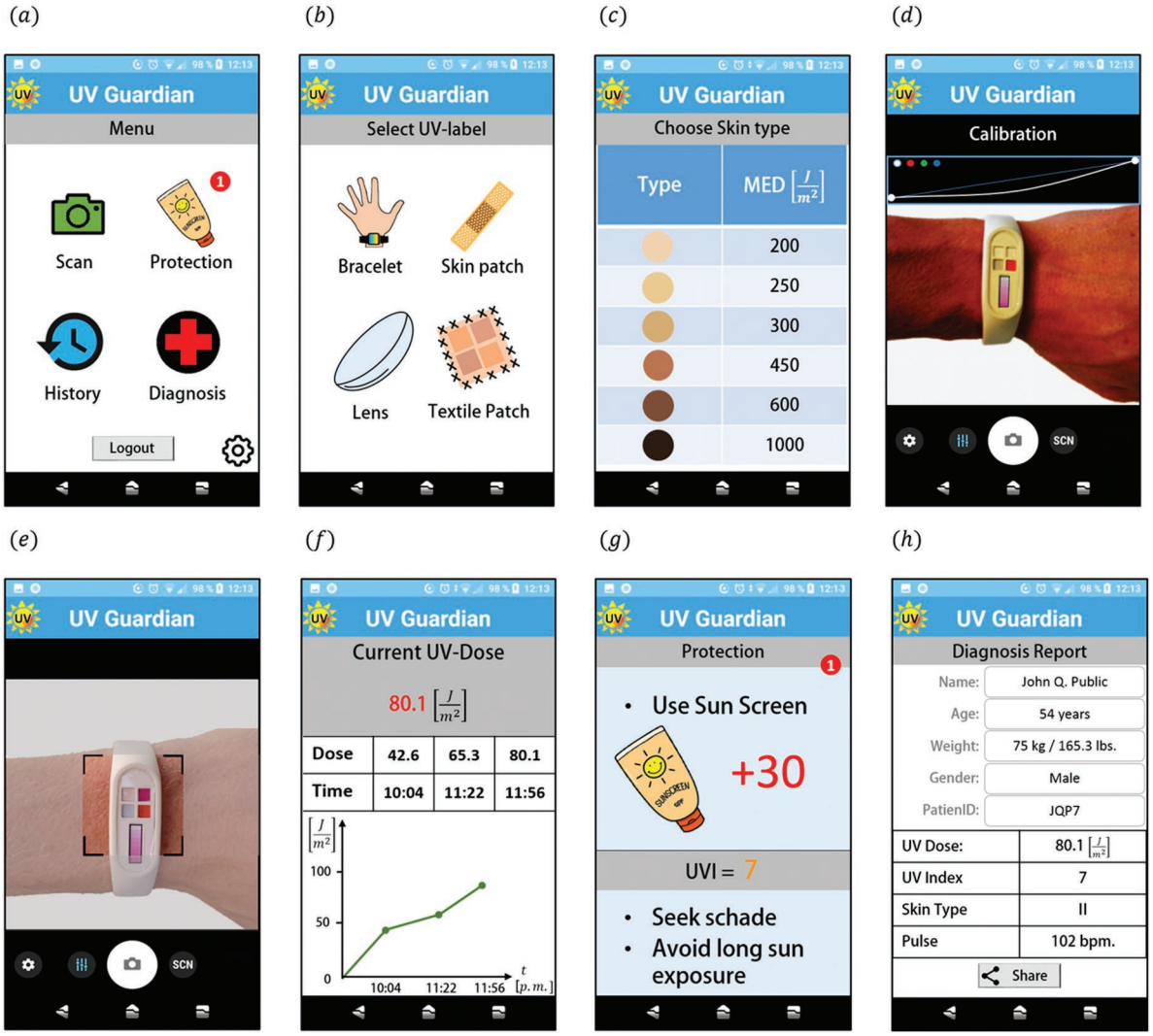


**Figure 7.** Smartphone readout algorithm utilizes the CMOS camera. a) Home screen with the option to scan a wearable device, view suggested protection methods, display the scan history and a diagnosis report. b) Selection of a UV-label from a bracelet, skin patch, contact lens, and textile patch. c) Choosing skin tone. d) Color and brightness compensation under ambient light. e) Scanning a UV-label (bracelet). f) The history of recorded values and graphical illustration of the measurement results. g) Suggested protection method based on the UV-dose and live UV index. h) Diagnosis report of specific user information and option to share data with a dermatologist.

$$\begin{bmatrix} X \\ Y \\ Z \end{bmatrix} = [M] \begin{bmatrix} r \\ g \\ b \end{bmatrix} \quad (1)$$

This allows the determination of the user's current UV dose through the nearest neighbor classification of the *XYZ* values (Figure 7e).[16] The specific UV light exposure dose and pre-measured values are displayed as a trend curve over time to illustrate the user's exposure to UV radiation (Figure 7f). In the protection section, the smartphone application suggests protection methods based on the skin type and the performed scans (Figure 7g). Additionally, the user can obtain a live request of the latest UV index on the radiation level at the specific location. The diagnosis function allows to track the recorded data with other vital parameters and share them with a dermatologist (Figure 7h).

UV-sensitive dyes show a promising method for monitoring UV radiation, comparable with other reported approaches.[17–19] However, most approaches in the literature are based on an evaluation of the colors without a smartphone application. One approach used UV dyes applied as smileys on a substrate, which change their smile with increasing exposure.[17] In another approach, the UV sensors were adapted to different skin types. By applying attenuating layers upon the sensor, the exposure time of the UV dyes was increased and adapted to darker skin types.[18] By using a smartphone application in combination with a reference scale (Figure 6a–c), personalization of the sensor to a specific skin type have practical applications since the UV dyes are designed for 1000 J $m^{-2}$ (1000 MED). By determining the skin type once in the application, the user receives the limit of his daily UV dose. For example, a person of skin type II would have a maximum dose of 250 J $m^{-2}$ (250 MED) before skin damage

occurs, which corresponds to exactly one quarter on the reference scale in Figure 6c. Additionally, the scan of a label through the smartphone application provides precise results of the current dose than visual evaluation. Based on these results, the user will receive preventative instructions displayed on the screen to avoid damage to the epidermis. Furthermore, it is possible to reuse an already used UV label at a later date, if the maximum exposure or transformation has not been reached. Accordingly, when a new UV label is scanned, the first color value obtained can be reset regardless of whether it has already been used or not.

## 5. Conclusion

The samples IS300, IS101, UV-label H, and UV-label M were found to be robust for variable device use. Nevertheless, for low intensities of 37.0 up to 85 mW $m^{-2}$, fast color transformations were noted within 30–300 min; therefore, UV blocking sunscreens could be used in combination with these dyes to extend their lifetime for a possible reuse. The use of UV-filtering films such as titanium dioxide ($TiO_2$) and zinc oxide (ZnO)[20] are suitable for the coating of the UV-dyes and can block up to 99% of UV-radiation while VIS-radiation is passing,[21] which allows for a controlled extension of device life time.

The toxicity of the reagents should be evaluated to ensure that the optical sensors are biocompatible and suitable for the use in skin or applied on a contact lens. Additionally, recyclable materials (thermoplastics) can be utilized to minimize the environmental impact by avoiding disposal and also brings advantages like corrosion resistance, low density, high strength, and user-specific designs.[18] For example, in case of a wristband, the insert can simply be replaced after use and the wasted material can be recycled. Furthermore, by integrating electronic sensors in the wearable devices presented in this work, biomarker in human sweat can be monitored in combination with UV sensing for application in personalized medicine. For example, diagnosis to the hydration state[24] or diseases like cystic fibrosis or diabetes[25] can be made by the electrochemical sensor applied on the back of the portable device with contact to the skin to indicate the current state of specific biochemical parameters with colorimetric responses.[26]

The present work allows for a colorimetric evaluation of UV sensitive dyes using smartphone applications to determine the user's UV-radiation dose and may have application in daily sun protection as well as dermatological sectors to prevent skin damage caused by solar radiation.

## Supporting Information

Supporting Information is available from the Wiley Online Library or from the author.

## Acknowledgements

This research was funded by the Alexander von Humboldt Foundation and Carl Friedrich von Siemens Foundation. M.J.F. thanks the Engineering and Physical Sciences Research Council for an Established Career Fellowship (EP/R00188X/1).

## Conflict of Interest

The authors declare no conflict of interest.

## Author Contributions

A.K.Y. conceived the idea. W.K. designed and carried out the experiments. A.K.Y. and W.K. analyzed the data. W.K., M.J., M.E., M.V.K., M.J.F., and A.W.K made intellectual contribution and wrote the article.

## Keywords

colorimetric sensors, dermatology, inks, photonics, UV dyes

Received: November 24, 2019
Published online: January 17, 2020

[1] M. F. Holick, *Anticancer Res.* **2016**, *26*, 1345.
[2] B. L. Diffey, *Methods* **2002**, *28*, 4.
[3] *Environmental Effects and Interactions of Stratospheric Ozone Depletion, UV Radiation, and Climate Change*, 2018 Assessment Report. Environmental Effects Assessment Panel, United Nations Environment Programme (UNEP), Ozone Secretariat, Nairobi, Kenya **2019**, p. 390.
[4] B. Barnes, K. Kraywinkel, E. Nowossadeck, I. Schönfeld, A. Starker, A. Wienecke, U. Wolf, *Bericht zum Krebsgeschehen in Deutschland 2016*, Robert Koch-Institut, Berlin, Germany **2016**, pp. 53–56.
[5] V. D. Ryzhikov, G. M. Onyshchenko, C. F. Smith, O. D. Opolonin, O. K. Lysetska, L. A. Piven, I. M. Zenya, O. V. Volkov, E. F. Voronkin, S. N. Galkin, I. Bendeberia, K. Katrunov, in *Proc. SPIE 7715, Biophotonics: Photonic Solutions for Better Health Care II* **2010**, pp. 321–331.
[6] D. Pines, E. Pines, *Biomed. Eng. Online* **2017**, *16*, 119.
[7] R. McKenzie, D. Smale, M. Kotkamp, *Photochem. Photobiol. Sci.* **2004**, *3*, 252.
[8] T. Iwata, K. Kinashi, H. N. Doan, P. P. Vo, W. Sakai, N. Tsutsumi, *ACS Omega* **2019**, *4*, 9946.
[9] J. Wang, A. S. Jeevarathinam, A. Jhunjhunwala, H. Ren, J. Lemaster, Y. Luo, D. P. Fenning, E. E. Fullerton, J. V. Jokerst, *Adv. Mater. Technol.* **2018**, *3*, 252.
[10] C. H. Ajith, R. M. G. Rajapakse, W. Anura, K. Veranja, *Environ. Sci. Technol.* **2009**, *43*, 176.
[11] J. V. Crivello, *J. Polym. Sci., Part A: Polym. Chem.* **1999**, *37*, 4241.
[12] International Commission on Illumination, *CIE 15: Technical Report: Colorimetry*, 3rd ed., Vienna, Austria **2004**, pp. 10–12.
[13] M. D. Fairchild, *Color Appearance Models*, 3rd ed., John Wiley & Sons, Ltd., New York **2013**, pp. 1–34.
[14] A. Volkov, in *Encyclopedia of Membranes*, Vol. *1*, (Eds: E. Drioli, L. Giorno), Springer, Berlin, Heidelberg **2013**, pp. 1–2.
[15] V. M. Rai, D. S. Shruthakithi, B. Chandrashekaran, B. P. Satish, *Indian J. Dermatol. Venereol.* **2004**, *70*, 277.
[16] P. Cunningham, S. Delany, *Mult. Classif. Syst.* **2007**, *34*, 1.
[17] W. Zou, A. González, D. Jampaiah, R. Ramanathan, M. Taha, S. Walia, S. Sriram, M. Bhaskaran, J. M. Dominguez-Vera, V. Bansal, *Nat. Commun.* **2018**, *9*, 3743.
[18] M. E. Lee, A. M. Armani, *ACS Sens.* **2016**, *1*, 1251.
[19] P. S. Khiabani, A. H. Soeriyadi, P. J. Reece, J. J. Gooding, *ACS Sens.* **2016**, *1*, 775.

[20] N. Serpone, D. Dondi, A. Albini, *Inorg. Chim. Acta* **2007**, *360*, 794.
[21] S. Samantha, *WAAC Newslett.* **2008**, *30*, 16.
[22] E. B. Manaia, R. C. K. Kaminski, M. A. Corrêa, L. A. Chiavacci, *Braz. J. Pharm. Sci.* **2013**, *49*, 201.
[23] E. G. Mădălina, *Recycling* **2017**, *2*, 24.
[24] P. Salvo, F. Di Francesco, D. Costanzo, C. Ferrari, M. G. Trivella, D. De Rossi, *IEEE Sens. J.* **2010**, *10*, 1557.
[25] S. Jadoon, S. Karim, M. Rouf Akram, A. K. Khan, M. A. Zia, A. R. Siddiqi, G. Murtaza, *Int. J. Anal. Chem.* **2015**, *2015*, 164974
[26] A. Koh, D. Kang, Y. Xue, S. Lee, R. M. Pielak, J. Kim, T. Hwang, S. Min, A. Banks, P. Bastien, M. C. Manco, L. Wang, K. R. Ammann, K.-I. Jang, P. Won, S. Han, R. Ghaffari, U. Paik, M. J. Slepian, G. Balooch, Y. Huang, J. A. Rogers, *Sci. Transl. Med.* **2016**, *8*, 366ra165.